



**A multitemporal and non-parametric approach for assessing the impacts of drought on vegetation greenness
a case study for Latin America**

Carrao, Hugo; Sepulcre, Guadalupe; Horion, Stéphanie Marie Anne F; Barbosa, Paulo

Published in:
E A R Se L eProceedings

Publication date:
2013

Document version
Publisher's PDF, also known as Version of record

Citation for published version (APA):
Carrao, H., Sepulcre, G., Horion, S. M. A. F., & Barbosa, P. (2013). A multitemporal and non-parametric approach for assessing the impacts of drought on vegetation greenness: a case study for Latin America. *E A R Se L eProceedings*, 12(1), 8-24. http://www.e proceedings.org/static/vol12_1/12_1_carrao1.html

A MULTITEMPORAL AND NON-PARAMETRIC APPROACH FOR ASSESSING THE IMPACTS OF DROUGHT ON VEGETATION GREENNESS: A CASE STUDY FOR LATIN AMERICA

Hugo Carrão¹, Guadalupe Sepulcre¹, Stephanie Horion^{1,2}, and Paulo Barbosa¹

1. European Commission (EC), Joint Research Centre (JRC), Institute for Environment and Sustainability (IES), TP280, I-21027 Ispra (VA), Italy;
e-mail: {[hugo.carrao](mailto:hugo.carrao@jrc.ec.europa.eu) / [guadalupe.sepulcre](mailto:guadalupe.sepulcre@jrc.ec.europa.eu) / [paulo.barbosa](mailto:paulo.barbosa@jrc.ec.europa.eu)}@jrc.ec.europa.eu
2. University of Copenhagen, Department of Geography & Geology, Øster Voldgade 10, DK-1350 Copenhagen K, Denmark; e-mail: stephanie.horion@geo.ku.dk

ABSTRACT

This study evaluates the relationship between the frequency and duration of meteorological droughts and the subsequent temporal changes on the quantity of actively photosynthesizing biomass (greenness) estimated from satellite imagery on rainfed croplands in Latin America. An innovative non-parametric and non-supervised approach, based on the Fisher-Jenks optimal classification algorithm, is used to identify multi-scale meteorological droughts on the basis of empirical cumulative distributions of 1, 3, 6, and 12-monthly precipitation totals. As input data for the classifier, we use the gridded GPCC Full Data Reanalysis precipitation time-series product, which ranges from January 1901 to December 2010 and is interpolated at the spatial resolution of 1° (decimal degree, DD). Vegetation greenness composites are derived from 10-daily SPOT-VEGETATION images at the spatial resolution of 1/112° DD for the period between 1998 and 2010.

The time-series analysis of vegetation greenness is performed during the growing season with a non-parametric method, namely the seasonal Relative Greenness (*RG*) of spatially accumulated *fAPAR*. The Global Land Cover map of 2000 and the GlobCover maps of 2005/2006 and 2009 are used as reference data to select study cases only on geographic areas that did not undergo land cover changes during the analysis period. The multi-scale information is integrated at the lowest spatial resolution available, i.e. 1° DD, and the impacts of meteorological drought episodes on seasonal greenness of rainfed crops are assessed at the regional scale. Final results suggest that the agricultural cycle at the regional scale is more correlated with long-standing and uninterrupted small timescale drought conditions that occur prior to vegetation growing season than with isolated and short long-term timescale drought events.

INTRODUCTION

Drought originates from a below average precipitation deficit that results in water shortage for natural processes (e.g. plant growth) and human activities (e.g. agriculture). Regardless of the environment, a lack of precipitation over a certain period of time and particular region may result in reduced quantity of actively photosynthesizing biomass (hereafter greenness) on the vegetation cover. When drought conditions end, recovery of living vegetation to normal conditions may follow, but such a recovery process may be slow and last for longer periods of time. In natural ecosystems, long-term dry conditions cause vegetation to be more prone to forest fires, while in human-induced ecosystems they reduce the fodder available for animals and the agricultural yield, thus leading to a reduction in income.

The usefulness of satellite imagery for monitoring vegetation vigour and phenology has been demonstrated (1,2). Indeed, the availability of remote sensing data covering wide regions over long periods of time has progressively strengthened the role of vegetation indices in environmental

studies related to drought episodes (3,4,5,6,7,8,9,10). In this context, there is an increased use of satellite images to directly monitor spatially-explicit patterns of drought-related changes in vegetation conditions (i.e. agricultural drought) in areas where weather stations are sparse or non-existent (5,11). However, it is impossible to rely solely on satellite-derived information to monitor drought, assess its duration and evaluate its impacts on living vegetation cover. The problem is that relatively poor vegetation conditions may be caused by factors other than drought, e.g. unseasonable coolness, crop rotation or wildland fires. Thus, as shown by (5,11), some additional background information on meteorological drought onset and end, derived from rainfall data recorded by meteorological networks, and updated information on land cover changes are a priori demanded for agricultural drought assessment. Indeed, the use of spectral remote sensing data to assess the greenness conditions of vegetated cover types over time must be restricted to real meteorological drought-related episodes, as agricultural drought is understood as a precipitation shortage sufficient to adversely affect vegetation growth (12).

Many authors evaluated the relationship between abnormal precipitation conditions estimated from rainfall gauge stations and the conditions of living vegetation estimated from remote sensing data at simultaneous times or at some fixed time lags, e.g., (7,9) to cite but a few. However, the correlations attained between meteorological droughts and vegetation indices are many times insignificant (e.g. only 3% to 15% of the individuals show a correlation higher than 0.4 in (9)) and can be explained simply by looking at the phenomenon from a discrete and near-real time viewpoint. Because a single isolated monthly meteorological drought occurs during the vegetation growing season, it does not imply a straightforward impact on its greenness. Indeed, one atypical monthly precipitation record can represent simply a shot noise in the dataset or be just a sporadic phenomenon without consequences for the normal development of vegetation.

On the other hand, it is also possible that vegetation stress continues after the end of a meteorological drought *sensus stricto* and still be associated to it. The complex cause-effect relationship between soil moisture deficit and vegetation stress is preponderant on short term drought occurrences and depends critically on associated variables and nonlinear processes of infiltration, evaporation, transpiration, and drainage (13). Correlating indiscriminately all meteorological and biophysical events without understanding their duration and time dependence (e.g. comparing weekly vegetation greenness with monthly precipitation records), can result in non-linear and incomprehensible relationships. Indeed, (14) highlighted that the vegetation development is not influenced by the intensity of the meteorological drought, but by its duration. Similarly, (12) stated that “the longer the rainfall deficiency is, the more likely other types of droughts [agricultural and hydrological] will occur as a result”. So, before using vegetation indices derived from satellite images to monitor the broadening patterns of agricultural drought, it is important to know how and when low rainfall supplies impact on the expected vegetation growth.

In this paper, we aim at evaluating the regional cause-effect relationship between below average precipitation deficits and consequent vegetation greenness anomalies estimated from remote sensing data during the growing season. In detail, our goal is to define the meteorological drought parameters, namely time of onset, duration and timescale of precipitation deficit that are able to impart a priori knowledge on the expected growth conditions of specific rainfed crops at the regional scale. This information is lacking in the literature and it is an important structural foundation for any monitoring system that aims at following (agricultural) drought events from time-series sets of vegetation indices derived from satellite imagery.

INPUT DATA

The data used to perform this study are divided in:

- a) existing global land cover maps used as complementary information for reference land cover type's identification and study area selection;

- b) a time series set of *fAPAR* (fraction of photo-synthetically active radiation absorbed by the canopy) estimates used for Relative Greenness (RG) computation; and
- c) a gauge-based gridded monthly precipitation dataset used for meteorological drought estimation. The details on the use of these data can be found on the next sections, i.e. Study Area Selection and Methodology.

Global land cover maps

The Global Agricultural Lands in the Year 2000 data set (GAL 2000).

This map shows the extent and intensity of agricultural land use on Earth. In detail, GAL 2000 represents the proportion of land area used as cropland (land used for the cultivation of food) and pasture (land used for grazing) in the year 2000. Satellite data from the Moderate Resolution Imaging Spectroradiometer (MODIS) and Satellite Pour l'Observation de la Terre (SPOT) Image Vegetation sensor were combined with agricultural inventory data to create a global data set. The data were compiled by (15) and are provided in raster GeoTiff and ESRI Grid formats, with a raster cell size of 5", or 0.08333° DD (about 10 kilometers at the equator).

The Land Cover of the World in the Year 2000 (Global Land Cover 2000, GLC 2000).

The GLC 2000 was developed by the Joint Research Centre (JRC) for the baseline year of 2000, which is a reference year for environmental assessment. The product was created using 14 months of pre-processed daily global data at a spatial resolution of 1 km, acquired by the VEGETATION instrument on board the SPOT 4 satellite. A bottom-up approach to product development was undertaken in which more than 30 research teams around the world contributed to 19 regional windows (16). The regional legends were derived from the United Nations (UN) Land Cover Classification System (LCCS) as a common framework to produce 22 global classes (17).

The Globcover Land Cover maps of 2005/2006 and 2009.

GlobCover is an European Space Agency (ESA) initiative to develop an automatic and regionally-tuned classification system to produce a global land cover map for 2005/6, using 300 meters resolution time series of image mosaics acquired globally by the MERIS sensor on board the ENVISAT satellite (18). This product was intended to update and to complement the other existing comparable global products – GLC 2000 in particular – and to improve on their spatial resolution. The global Globcover legend is compatible with the GLC2000 global land cover classification and similarly comprises 22 land cover classes that were also defined with the UN LCCS. GlobCover 2009 was released in December 2010 and produced with a time series set of MERIS images for the year 2009; its legend is identical to that of the GlobCover 2005/2009, thus being compatible also with the GLC2000 global land cover classification.

fAPAR

fAPAR is the fraction of photosynthetically active radiation (400-700 nm) absorbed by green vegetation. It is one of the Essential Climate Variables recognized by the UN Global Climate Observing System (GCOS) as of great potential to characterize the climate of the Earth (19). Due to its sensitivity to vegetation stress, *fAPAR* was already proposed as a drought indicator (9). The *fAPAR* product used in this study covers the period between 1st of April 1998 and 31st December of 2011 and is derived from VEGETATION sensors at 10 days temporal sampling (composited over 30-day windows) over 1/112° DD plate-carrée spatial grid (20). The 10-daily *fAPAR* composites (hereafter *fAPAR*) are assessed by inverting the SAIL radiative transfer model simulations through a supervised neural network that considers the solar zenith angle at 10 a.m. local time and the top of canopy nadir reflectances in the red, NIR and SWIR wavebands (20). VEGETATION input reflectance wavebands are subjected to enhanced radiometric calibration, cloud screening, atmospheric correction and BRDF normalization (20), and are characterized by a multi-temporal registration uncertainty around 150 m (1 σ), which was measured by (21) and (22). The validation of the *fAPAR* products derived from VEGETATION was performed by (23) and the results show a very

good temporal consistency with the MODIS collection 4.1 *fAPAR*, thus providing a clear characterization of vegetation seasonality. Moreover, the VEGETATION *fAPAR* product was compared with *in situ* measurements collected over experimental sites of ground networks and a good agreement of RMSE ≈ 0.10 within the magnitude of product values was verified (23).

A gauge-based gridded monthly precipitation

The precipitation data used in this study is derived from the Global Precipitation Climatology Centre (GPCC) Full Data Reanalysis Monthly Product Version 6 for the Latin America region at 1° (DD) grid and the long-term period of January 1901 – December 2010. The GPCC has been established in 1989 and provides a global analysis of monthly precipitation on Earth's land surface based only in situ rain gauge data. The data supplies from 190 worldwide national weather services to the GPCC are regarded as primary data source, comprising observed monthly totals from more than 65,000 stations since 1901 (24). All GPCC monitoring products are available in a monthly basis at the spatial resolutions ranging from 1.0°×1.0° to 2.5°×2.5° (decimal degrees); non real-time products are also available in 0.5°×0.5° resolution. GPCC is operated by Deutscher Wetterdienst (DWD) under the auspices of the World Meteorological Organization (WMO).

STUDY AREA SELECTION

We focus our experiences in Latin America because it has been extremely affected by drought events in the past (25,26,27) and the climate change scenarios foresee an increased frequency of these events in the region (28,29). In addition, the extensive plains located in middle and subtropical latitudes of Latin America are within the main areas that produce cereals worldwide (e.g. Brazil and Argentina) (30), thus constituting an excellent use case study for testing our assumptions, as we explain hereafter.

Before describing in detail the methodological approach for selecting the final study area, we first explain that the spatial resolution of the statistical analysis performed within this study equals the coarsest dataset, i.e., the GPCC precipitation grid cell at 1° DD, which comprises 12544 *fAPAR* pixels over 1/112° spatial resolution. From the viewpoint of climate and weather variability, we assume that 1° DD spatial resolution is detailed enough to guarantee the homogeneity of monthly precipitation regimes inside its boundaries and that all *fAPAR* pixels are affected similarly by the estimated precipitation deficits. Indeed, this assumption stands as we are not interested in precision farming or intra-field agricultural variations, but on average regional impacts of low precipitation deficits, i.e. meteorological droughts. Moreover, a study area with 1° DD spatial resolution is large enough to study the correlation between reduced green vegetation cover and precipitation deficits at the regional scale.

To assess the hypothesis that the growing conditions of rainfed crops correlate with preceding precipitation deficits at the regional scale, i.e. meteorological droughts, we aim at selecting a geographical window containing a high percentage cover of rainfed crops and few temporal land use/ land cover changes (LULCC) in the period between 1st of April 1998 and 31st December of 2010. To undertake this selection task, we first overlaid the *GAL 2000* product with the GPCC fishnet and identify the 1° DD cell in Latin America region with the highest proportion of land area covered by rainfed crops in the year of 2000. In the sequence, and to avoid that the examined vegetation dynamics are biased by LULCC, we constrained the study area to the rainfed croplands that did not undergo LULCC during the analysis period inside the pre-selected cell. To perform this spatiotemporal stratification, we used the *GLC2000* and the *GlobCover* maps of 2005/2006 and 2009 as reference data. The stratification process ensured that the final study area is characterised only by a set of multi-temporal stationary rainfed croplands.

Finally, the selected study area corresponds to a 1° DD grid cell, located in *Cañada de la Mala Cara*, Córdoba Province, Argentina (Figure 1a). According to the areal estimates based on the ancillary global land cover maps presented in the Input Data section, 87% of the study area was occupied by rainfed crops in 2000 (Figure 1b), from which only 5% undergo land cover changes

between 2000 and 2009. The final study area (Figure 1c in green) is characterized by large agricultural areas that are occupied mainly by soya bean crops, wheat crops and other cash crops that grow normally between December each year and February next year (30,31).

METHODOLOGY

This section describes in detail the seasonal Relative Greenness (RG) computation, the meteorological drought estimation and the correlation analysis used to evaluate the relationship between RG and meteorological drought conditions. We focus our correlation analysis on the period between April 1998 and December 2010, as this is the overlapping time between the available precipitation and vegetation datasets.

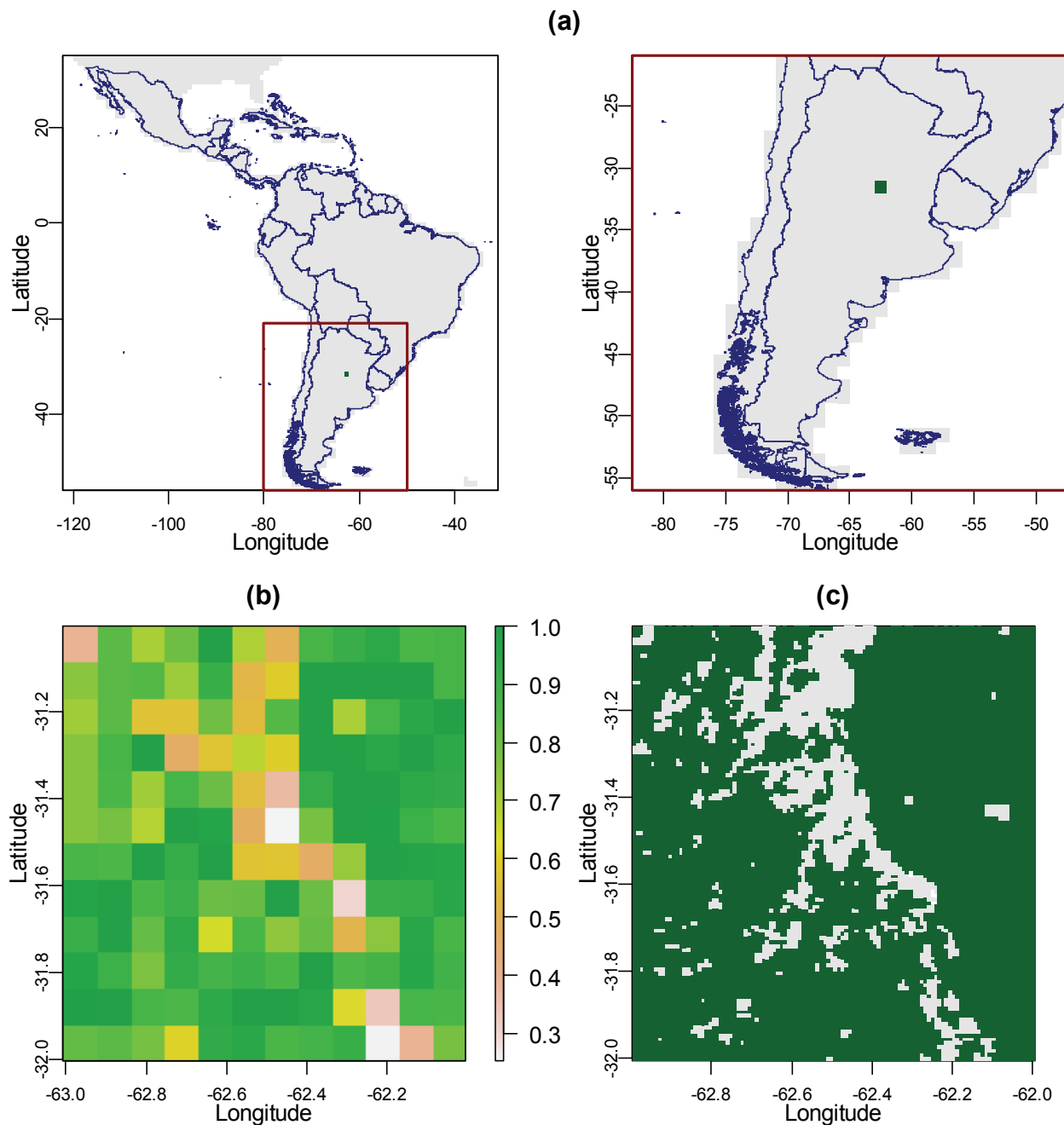


Figure 1: a) The study area (green square) in Latin America region (left panel) and Argentina (right panel); b) percentage of rainfed crops in 2000 (mapped from GAL 2000); c) the agricultural area that did not undergo changes between 2000 and 2009 (in green).

Relative Greenness (*RG*) computation

A modified version of the Relative Greenness (*RG*) index (32) is used here to estimate the unconditional greenness conditions of rainfed crops during the growing season in the study area. The *RG* (32) was originally defined as a percentage value that expresses for each geographic location the conditions of the living vegetation in relation to the upper and lower limits of the “normal” ecosystem resources in that point (4). It varies between 0 and 1, reflecting changes in the vegetation conditions from, respectively, extremely bad to optimal. The ecosystem limits have been estimated relatively to the maximum and minimum observed historical values of a vegetation index (*VI*), namely the Normalized Difference Vegetation Index (*NDVI*), and are commonly computed from remote sensing spectral data. The concept of *RG* is the same as the “Vegetation Condition Index (*VCI*)” (3). However, the former is normalized for a specific intra-annual period (usually 10-daily, biweekly or monthly) on the basis of the minimum and maximum *VI*s’ values estimated for each geographic location from the historical multi-year satellite image records for that specific period. In this study, we use an approach based on (32), (3) and (4) and compute a seasonal relative greenness index ($RG_{GS,n}$) from *fAPAR* data for the growing period of rainfed crops in the whole study area. For the growing season (*GS*) in year *n*, the index is computed as follows:

$$RG_{GS,n} = \frac{(fAPAR_{GS,n} - fAPAR_{GS,min})}{(fAPAR_{GS,max} - fAPAR_{GS,min})} \quad (1)$$

where:

- $fAPAR_{GS,n}$ is the *fAPAR* accumulated for whole multi-temporal stationary rainfed croplands in the study area during the growing season (*GS*) in year *n*;
- $fAPAR_{GS,min} = \min\{fAPAR_{GS,n} : 1 \leq n \leq N\}$
- $fAPAR_{GS,max} = \max\{fAPAR_{GS,n} : 1 \leq n \leq N\}$;
- *N* is the total number of years covered by the *fAPAR* imagery dataset.

Please note that:

- (1) We focus our experiences on the pooled set of *fAPAR* pixels that correspond to stationary rainfed croplands within the study area, in opposition to the per-pixel analysis implemented as working strategy both by (32) and (3,4). We claim that individual per-pixel analysis is subject to higher radiometric and geometric noise, thus possibly biasing the correlation analysis between meteorological drought and vegetation stresses. In addition, and as stated before, the precipitation dataset that we are using is too coarse to evaluate the impact of precipitation deficits on within sub-study area sections. Smoothing the greenness variability within the study area by decreasing the resolution of the vegetation index pixels to the spatial resolution of GPCC data will reduce also the noise in the analysis caused by differences in the spatial resolution of used datasets.
- (2) We focus our experiences on seasonal accumulated *fAPAR* and not on 10-daily composites, because our goal here is to assess the response of average seasonal vegetation greenness to different precipitation deficits, i.e. meteorological droughts, occurring during the *a priori* growing season period, and not to monitor the temporal evolution of their interrelationship, if some.

To estimate $fAPAR_{GS,n}$, we need first to define a fixed intra-annual growing season (*GS*) for the rainfed crops in the study area. The definition of a common *GS* period is necessary to guarantee that differences in the members of the set $fAPAR_{GS} = \{fAPAR_{GS,n} : 1 \leq n \leq N\}$ are due only to impacts of abnormal precipitation conditions and not to differences in the length of the greenness accumulation periods for different years *n* in the database.

The GS period for the study area is defined here as the set of consecutive 10-daily periods in $GS = \{\cap_n GS_n : 1 \leq n \leq N\}$. GS_n equals the time period in year n where the median $fAPAR$ values computed for the whole rainfed crops in the study area are above the historical inter-annual empirical mean $fAPAR$, i.e., $GS_n = \{t : \overline{fAPAR}_{t,n} > \overline{fAPAR}; n \in [1, N]\}$. $\overline{fAPAR}_{t,n}$ represents the median $fAPAR$ value of rainfed crops in the study area for 10-daily composite t and year n , and \overline{fAPAR} represents the historical inter-annual empirical mean $fAPAR$ estimated over the whole croplands in the study area as:

$$\overline{fAPAR} = \frac{\max\{\overline{fAPAR}_n : 1 \leq n \leq N\} + \min\{\overline{fAPAR}_n : 1 \leq n \leq N\}}{2} \quad (2)$$

Meteorological drought estimation

Meteorological drought can be defined as “period of more than some particular number of days with precipitation less than some specified small amount” (33). Several classification systems characterizing meteorological drought onset and intensity have been published in the literature. Their advantages, added values, limitations and drawbacks have been already presented in numerous studies, e.g. (34,35). However, all of these classification systems prescribe fixed thresholds to identify precipitation conditions that correspond to meteorological droughts in a given time and location. Although these thresholds allow comparing drought trends of standardized frequencies between different geographical regions, they do not correspond to optimized physical boundaries of low precipitation regimes that are characteristic of local climate conditions. However, physically defined low precipitation regimes are a very important condition in the case of the intra-annual phenological development of vegetation. In fact, in regions where water availability is limiting vegetation growth, we expect vegetation greenness to respond to anomalies in the precipitation totals that are function of the characteristics of the climatology of the region and not to low rainfall regimes established with ad-hoc or operational thresholds.

In this study, we propose an innovative method to identify monthly meteorological drought events based on precipitation time series alone and the Fisher-Jenks optimal classification algorithm. Similarly to many other approaches (36,37), we currently adopt the median of historical precipitation totals for each month and geographical point as the “normal” climatological precipitation conditions for that particular combination. Because the distribution of precipitation data is often skewed and sometimes has heavy tails, the median is generally considered to be the sample statistic best representative of its central location (38). Besides the estimation of the long-term median as the reference value for the computation of rainfall deviations to normal water supply conditions, it is also necessary to determine a scientifically justified band around this reference that separates drought from recurring temporary dry spells. Because drought conditions are more extreme and less frequent than “below normal” conditions, then within this band the precipitation fluctuations should be considered to be normal, whereas beyond it may be considered abnormal (or exceptional). In opposition to current drought intensity classification schemes that are based on fixed truncation boundaries (or fixed thresholds), our method adapts to the characteristics of empirical precipitation frequencies in the region and allows to determine the boundary below the median that optimally separates between “drought” and “non-drought” like precipitation observations.

Meteorological droughts are estimated on a monthly basis at the 1° DD spatial resolution for the Latin America region from the GPCC precipitation data. In detail, for each GPCC grid cell k in the study area and month $j = 1, \dots, 12$, we first compute the median precipitation value $\widetilde{P}_{k,j}$ from the 110 available yearly records and identify the years $N_{-1,k,j}$ in the respective time-series where the monthly precipitation values are less than or equal to the estimated median, as $N_{-1,k,j} = \{n : P_{k,j,n} \leq \widetilde{P}_{k,j}; 1 \leq n \leq N\}$, where N is now the total number of years covered by the

precipitation dataset. In the sequence, we use the Fisher-Jenks classification algorithm to optimally allocate the set of precipitation records $P_{-1,k,j} = \{P_{k,j,n}; n \in N_{-1,k,j}\}$ into two groups:

- 1) the set of observations $P_{d,k,j} = \{P_{k,j,n} \approx \min\{P_{-1,k,j}\}; n \in N_{-1,k,j}\}$; and
- 2) the set of observations $P_{\bar{d},k,j} = \{P_{k,j,n} \approx \widetilde{P}_{k,j}; n \in N_{-1,k,j}\}$.

Similarly, we can apply the classification process to the remaining precipitation individuals in the original time-series, i.e. $P_{1,k,j} = \{P_{k,j,n}; n \in N_{1,k,j}\}$, where $N_{1,k,j} = \{n: P_{k,j,n} > \widetilde{P}_{k,j}; n \in N_{-1,k,j}\}$, and distribute them into the following two groups:

- 1) the set of observations $P_{w,k,j} = \{P_{k,j,n} \approx \max\{P_{1,k,j}\}; n \in N_{1,k,j}\}$; and
- 2) the set of observations $P_{\bar{w},k,j} = \{P_{k,j,n} \approx \widetilde{P}_{k,j}; n \in N_{1,k,j}\}$.

From a semantic view point, $P_{d,k,j}$ are the only individuals that can be considered in “physical” meteorological drought, as they approximate the minimum precipitation total that was ever registered for region k and month j between 1901 and 2010.

On the other hand, the groups of observations $P_{\bar{d},k,j} = P_{d,k,j} \cup P_{\bar{w},k,j}$ and $P_{w,k,j}$ are closer or above, respectively, to the expected precipitation value for the region and thus cannot be physically considered in meteorological drought.

Finally, we create a discrete monthly time-series of drought and non-drought events for each grid cell k , as:

$$D_{k,j,n} = \begin{cases} -1 & \text{if } P_{k,j,n} \in P_{d,k,j} \\ 0 & \text{if } P_{k,j,n} \notin P_{d,k,j} \end{cases},$$

where $j = 1, \dots, 12$ months and $1 \leq n \leq N$ years. Note that similarly to other drought indices, $D_{k,j,n}$ can simultaneously be computed for different time-scales (i.e. precipitation accumulation periods), typically 3-, 6-, and 12-months. Short accumulation periods are useful for monitoring drought impacts on agricultural yields, while long-term accumulation timescales are important mainly for assessing impacts on reservoirs levels and groundwater supplies (39). In this paper, we evaluate also the potential usefulness of each drought timescale (i.e., 1-, 3-, 6-, and 12-months) for assessing the preceding weather conditions that may lead to major seasonal vegetation greenness anomalies at the regional scale.

Correlation analysis between relative greenness and meteorological drought

To verify the hypothesis that specific meteorological drought conditions relate to consequential decreases in seasonal RG values of rainfed crops, we also need to define the intra-annual period in which low precipitation regimes may affect the growth conditions of rainfed crops in the study area. We denominate this period as Precipitation Season for Vegetation Growth (PSVG) and define it as the set of months comprised between the starting of the rainfed crops growing season (see RG computation section) and the starting of the respective rainy season. Then, for each timescale of i -months (i.e. 1-, 3-, 6-, and 12-months) precipitation accumulation, we compute the seasonal indicator i -SD $_{k,n}$ that represents the summed $D_{k,j,n}$ during the PPVG in region k and year n . In addition, we compute two composite seasonal meteorological drought indicators, i.e. the total sum of seasonal meteorological droughts (TSD_k) and the weighted sum of seasonal meteorological droughts (T_wSD_k), both for region k and year n , as:

$$TSD_{k,n} = \sum_{PSVG} (i - SD_{k,n}), \quad i = 1, 3, 6 \text{ and } 12, \quad (3)$$

$$T_wSD_{k,n} = \sum_{PSVG} \frac{1}{i} \times (i - SD_{k,n}), i = 1, 3, 6 \text{ and } 12. \quad (4)$$

The weights defined for $T_wSD_{k,n}$ correspond simply to the inverse length of the precipitation timescale, as recent water supplies anomalies tend to higher impact the vegetation greenness of rainfed crops.

Finally, to test our hypothesis, we perform a correlation analysis with the Pearson coefficient for each year $n = 1998, \dots, 2010$, between the $RG_{GS,n}$ and each of the seasonal drought indicators proposed in this study, namely $i-SD_{k,n}$, $TSD_{k,n}$ and $T_wSD_{k,n}$.

RESULTS AND DISCUSSION

In Figure 2a one presents the empirical mean $fAPAR$ estimated for the study area and the median $fAPAR$ distribution along time, and in Figure 2b we compare the temporal distribution of the 25th, 50th and 75th $fAPAR$ percentiles for the study area. Two important points need to be detailed. First, we perceive that the land cover management practices vary along time, as the amplitude of the sinusoidal harmonic function that describes the median $fAPAR$ distribution along time increases from 1998 to 2011. Although an exhaustive process was performed to identify LULCC and remove possible outliers from the crops classification, it was not possible to remove changes in the agricultural practices. This shows how extremely difficult is to establish a system that depends on ancillary data, which is not always available or is not sufficiently detailed to support the necessary analysis. Secondly, we perceive that changes in the land use practices are similar along time for the whole study area, as the estimated interquartile distances are maintained (Figure 2b). This is an important point to retain, as it suggests that time changes in the weather conditions in the region will similarly impact the whole rainfed crop types inside the study area.

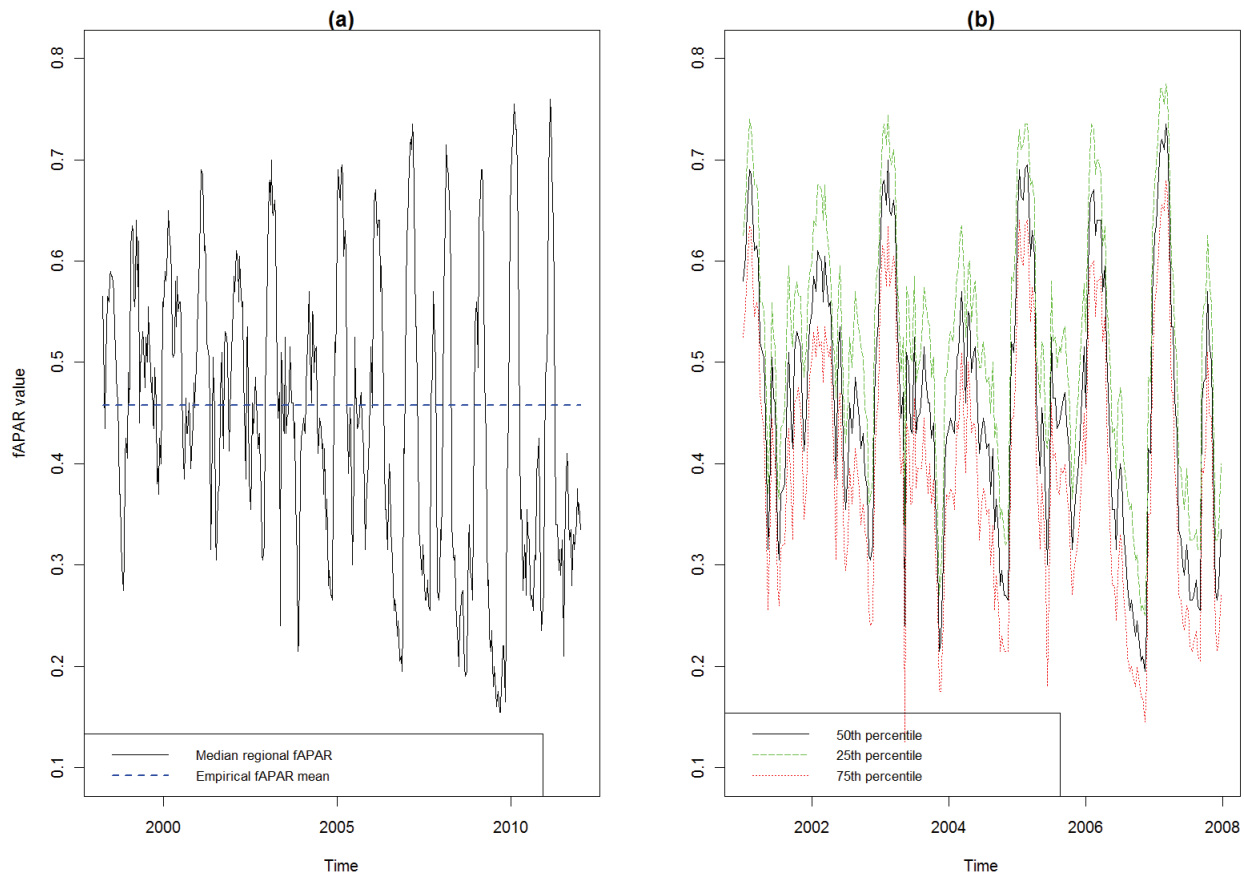


Figure 2: a) Empirical mean and median $fAPAR$ for the study area as function of whole available time; b) 25th, 50th and 75th $fAPAR$ percentiles for the study area between 2001 and 2008.

Based on the information presented in Figure 2, we defined the *GS* for the study area as the set of 10-daily periods comprised between 21st January and 1st of April each year. Because this growing period was relatively constant – just extending at a maximum of 2 more weeks in some of the years between 1998 and 2010 – it can be assumed that the crops in the study area present similar phenological cycles along the period of analysis and can be used for testing our hypothesis.

In Figure 3a, we present the accumulated *fAPAR* for each year (i.e. $fAPAR_{GS,n}$) and in Figure 3.b the respective seasonal relative greenness ($RG_{GS,n}$). In both diagrams of Figure 3 it is illustrated the remarkable anomaly affecting the greenness of agricultural crops in the region during the season of 2003-2004, as compared to the other seasons evaluated in the analysis. The first evidence is the continuous and notable increasing distance between the accumulated $fAPAR_{GS,03-04}$ (Figure 3a) and the *fAPAR* accumulated during the growing period of the remaining years evaluated in the analysis. Although from Figure 3a it is captured the intensity of the anomaly, from Figure 3b it is evident that the $RG_{s,03-04}$ is substantially inferior to that of the other years. This suggests for some phenomenon causing a notable disturbance in the normal development of the rainfed crops in the region.

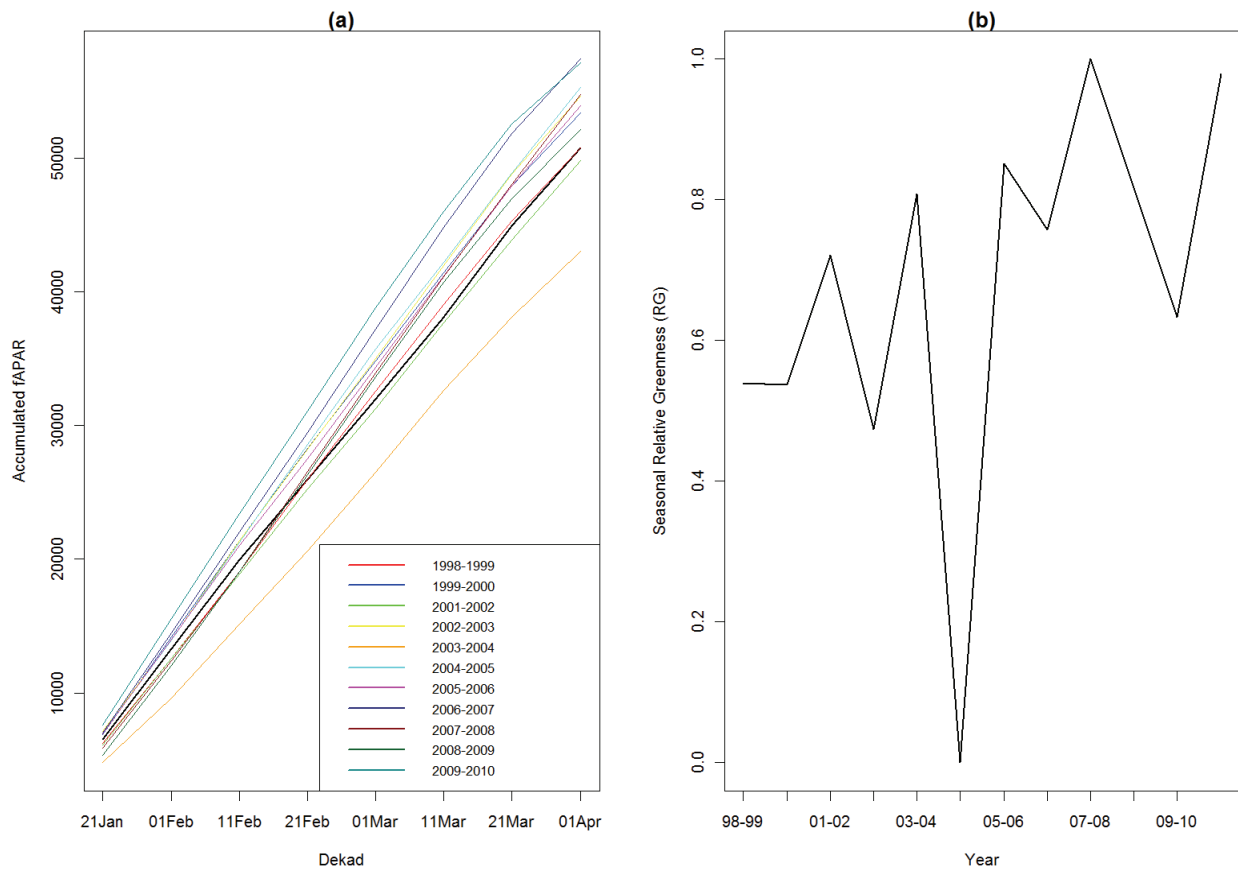


Figure 3: a) Accumulated $fAPAR_{GS,n}$ for different years along the decades of the growing season; b) $RG_{GS,n}$ computed for the years between 1998 and 2010.

Let us now look for some evidence between drought indices' values and the anomalous accumulated $RG_{GS,n}$ of rainfed crops during growing season of 2003-2004. In Figure 4a-d, we show the discrete time variation of monthly drought indices' values, $i-D_k$, computed for timescales of 1-, 3-, 6-, and 12-months precipitation accumulation. As expected, the number of discrete consecutive months' under drought becomes longer with the increase of the timescale of analysis, but the number of droughts occurring is smaller. Physically, this outcome verifies the validity of the proposed drought indicator, as from that viewpoint it is likely that small timescale monthly droughts recover faster than large timescale monthly droughts. In words, it takes physically more time to re-

establish the “normal” water supply conditions within a system where rainfall deficit increases during a long period than a short one.

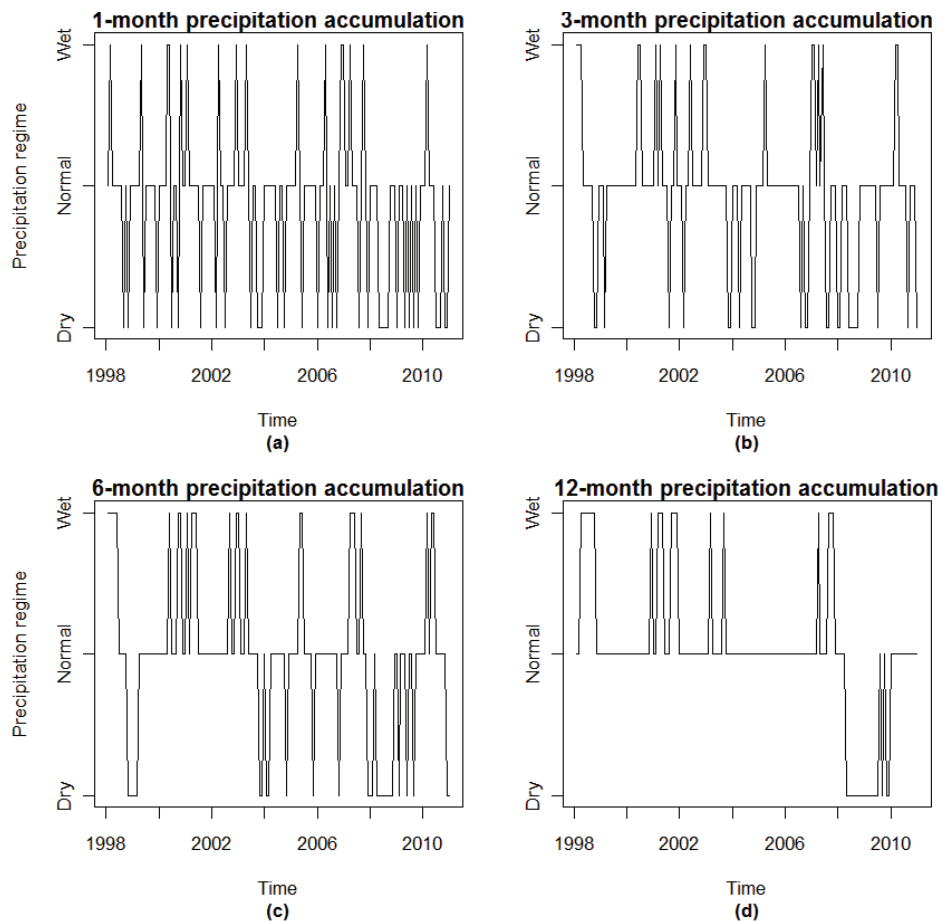


Figure 4: Monthly drought events as function of time for: a) $1-D_k$; b) $3-D_k$; c) $6-D_k$; d) $12-D_k$.

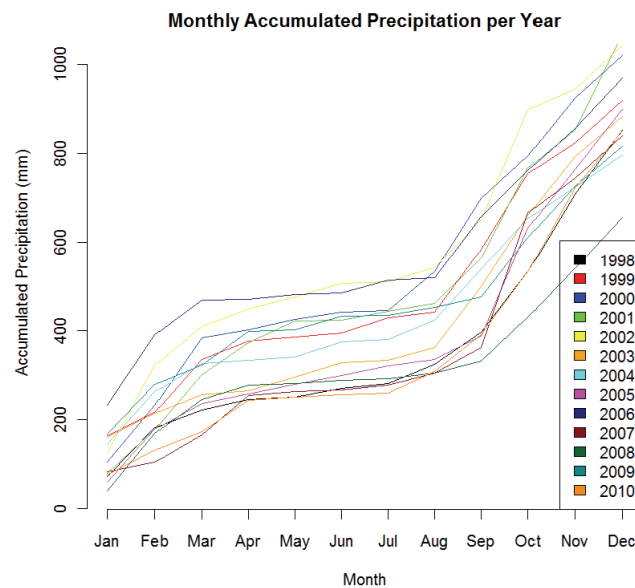


Figure 5: Intra-annual monthly accumulated rainfall for the years between 1998 and 2010.

As the discrete time variation of monthly drought occurrences for different timescales seems not to put in evidence the shortage on $RG_{GS,n}$ observed for the rainfed crops in the season of 2003-2004, it is now important to evaluate if consecutive monthly meteorological drought events relate to that

shortage. From Figure 5, which shows the intra-annual monthly accumulated rainfall for the years between 1998 and 2010, we perceive that the annual rainfall period averagely begins in September/October each year and ends by the end of March next year. Consequently, we define the *a priori* growing season period between October and December as the *PSVG* for the study area and use it to evaluate the impact of accumulated meteorological drought on the seasonal relative greenness of rainfed crops. Please recall that we defined January as the starting month of the growing season for rainfed crops in the study area.

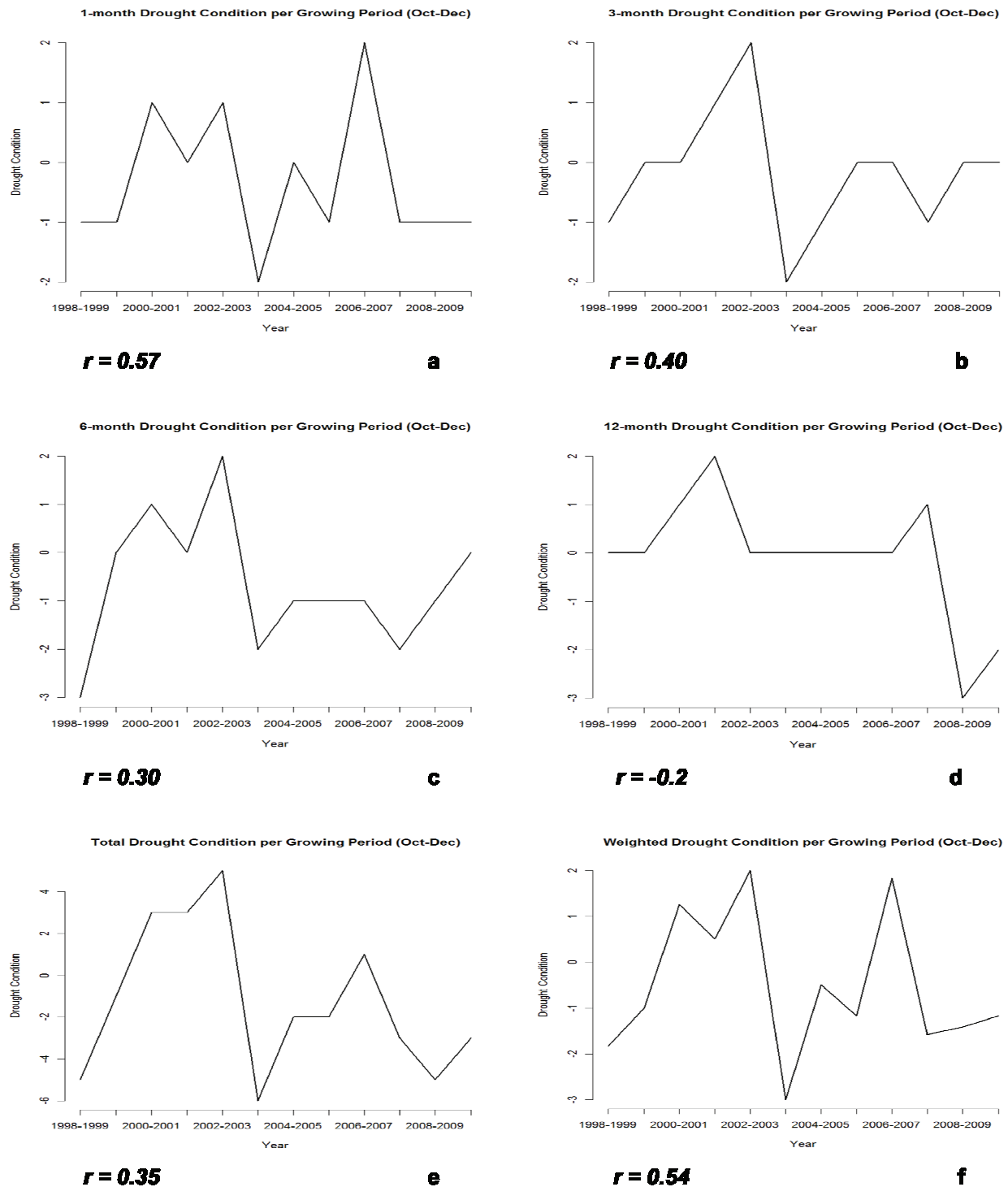


Figure 6: Accumulated monthly meteorological drought values for: a) $1-SD_k$; b) $3-SD_k$; c) $6-SD_k$; d) $12-SD_k$; e) TSD_k ; f) T_wSD_k .

In Figure 6a-f, we present the time distribution of accumulated drought indices' values for the seasons between 1998-1999 and 2009-2010, as well as the Pearson correlation coefficient (r) measuring the strength of the linear relationship between each indicator of accumulated drought and the $RG_{GS,n}$ presented in Figure 3b. From a general viewpoint, it is worth mentioning that all indicators, with the exception of 6-SD (Figure 6c) and 12-SD (Figure 6d), show a relevant drought event for the season 2003-2004, as measured by the accumulated drought indicator. This event matches the highest shortage on accumulated relative greenness for the study area. Indeed, according to (40) and (41), there was a remarkable meteorological drought in this season, that extended between January 2003 and March 2004 and largely affected the crops in the region. In fact, the crops in 2003 were not affected, as the rainfall deficit started after vegetation growing period. However, because there were continuous short timescale monthly droughts occurring in the PSVG period of 2003-2004, the crops in 2004 were affected.

In the sequence, we perceive also that there is a decrease in the correlation coefficient r as long as we increase the timescale (or precipitation accumulation period) of the accumulated drought indicator, i.e. from Figure 6a to 6d. This outcome suggests that short timescale, independent and continuous meteorological droughts occurring during the period preceding the time of vegetation growing are the type of precipitation shortage that most affects the normal phenological conditions of rainfed crops. The reasons are evident: on the one hand, large timescale droughts may be the result of independent and longstanding short timescale monthly droughts that are no longer affecting the vegetation conditions, but just now visible at a lower temporal resolution; on the other hand, the impacts of isolated monthly droughts are easily smothered by the system or may be a noise shot in the time-series and cannot be trustable.

Looking now at Figures 6e and 6f, i.e. the accumulated monthly drought values that combine all available timescales, we perceive again that small timescale drought patterns contribute more than those at larger timescales to a match with the seasonal relative greenness. Thus, these results also evidence that for an *a priori* evaluation of the impacts of meteorological droughts on seasonal vegetation greenness, it is more useful to rely on accumulated and consecutive short-term drought events than on larger and sporadic ones.

CONCLUSIONS AND RECOMMENDATIONS

In this paper we aimed at evaluating the cause-effect relationship between long-lasting meteorological droughts and the changes in regional vegetation greenness conditions during growing season period, which can serve as *a priori* structural information to predict the impacts of low precipitation supplies on the expected seasonal development of vegetation.

We extended the concept of seasonal accumulated relative greenness from pixel to regional level. The proposed indicator was evaluated on an agricultural region in Argentina, Latin America, which is mainly covered by soya bean and wheat rainfed crops. The indicator was computed from a time-series set of 10-daily fAPAR images derived from SPOT-VEGETATION data collected between 1998 and 2010. The results show that the proposed approach was successful on exposing the regional impacts of meteorological drought on the normal growth of rainfed crops in the study area, by accurately identifying the drought characteristics that affected the crop production in the region during the growing season of 2003-2004.

Meteorological drought events were estimated with an innovative and non-parametric classification technique that is based on the Fisher-Jenks algorithm. Its main advantage is the ability to adapt to the climatological characteristics of the geographical region when defining the drought thresholds from historical rainfall records. The results show a physical coherence between drought timescales and their average duration, thus giving us confidence on the validity of the indicator. Moreover, using the cumulative values of monthly droughts that precede the vegetation growing season as *a priori* knowledge for assessing its consequential greenness development, we were able to clearly identify in advance the decrease in the rainfed crops production in 2003-2004. In fact, the results

showed that the agricultural cycle is more correlated with long-standing and continuous small timescale drought conditions than with discrete or short long-term timescale drought events.

This study reports only the case of rainfed crops, but the results can also be associated with other types of vegetation, namely forest, shrubland and grassland. Similarly, it would be appreciated to confirm the relationship attained in this study for different study areas with the same land use/cover type, but different climatic and topographic conditions. In this study, we focused on *fAPAR* derived from SPOT-VEGETATION satellite images. Although the attained results are already extremely positive, there is still in the research community a long discussion about different vegetation indices and their usefulness for drought assessment and monitoring. It would be interesting to evaluate the behaviour of different data on this study case scenario in order to select the most adequate dataset to monitor agricultural drought events.

Regarding the estimation of drought, several improvements and modifications to the methodology can still be performed in order to improve it. The quality of input data should be optimized, as the number of stations used to compute GPCC products are highly variable in space and time. The spatial resolution of the input precipitation records can be enhanced with other datasets, namely Tropical Rainfall Measuring Mission (TRMM) remote sensing images. At this moment, the baseline statistics for characterizing the climatology of the region are based on a continuous period between 1901 and 2010. However, it is important to evaluate the impacts of the ENSO (El Niño Southern Oscillation) events on the baseline statistics for meteorological drought computation – and even on relative greenness estimation. Regarding the accumulated drought indicators, we think that a scheme with different weights can be tested and further optimized based on more detailed information about the weather variability in the region and phenological characteristics of different types of vegetation.

ACKNOWLEDGEMENTS

This work was funded by the EUROCLIMA Initiative Programme (N° DCI-ALA/2009/021-126) of the Directorate General for Development and Cooperation (DG DEVCO) of the European Commission (EC). Hugo Carrão thanks to Gustavo Naumann and Andrew Singleton for the important discussions about precipitation regimes and vegetation characteristics in Latin America. The authors are grateful to the two anonymous reviewers for their comments that greatly improved the quality of this work.

REFERENCES

- 1 Hill J, M Stellmes, T Udelhoven, A. Roder & S Sommer, 2008. Mediterranean desertification and land degradation mapping related land use change syndromes based on satellite observations. Global and Planetary Change, 64: 146-157
- 2 Wessels K, K Steenkamp, G von Maltitz & S Archibald, 2010. Remotely sensed vegetation phenology for describing and predicting the biomes of South Africa. Applied Vegetation Science, 11: 1-19. DOI: 10.1111/j.1654-109X.2010.01100.x
- 3 Kogan F N, 1990. Remote sensing of weather impacts on vegetation in non-homogeneous areas. International Journal of Remote Sensing, 11: 1405-1419
- 4 Kogan F N, 1997. Global drought watch from Space. Bulletin of the American Meteorological Society, 78(4): 621-636
- 5 Ji L & A Peters, 2003. Assessing vegetation response to drought in the northern Great Plains using vegetation and drought indices. Remote Sensing of Environment, 87: 85-98
- 6 Rhee J, J Im & G J Carbone, 2010. Monitoring agricultural drought for arid and humid regions using multi-sensor remote sensing data. Remote Sensing of Environment, 114: 2875-2887

- 7 Caccamo G, L A Chisholm, R A Bradstock & M L Puotinen, 2011. Assessing the sensitivity of MODIS to monitor drought in high biomass ecosystems. Remote Sensing of Environment, 115: 2626-2639
- 8 Horion S, P Barbosa, K Kurnik & J Vogt, 2010. Comparison of remote sensing and meteorological drought monitoring indicators in the Greater Horn of Africa (extended abstract). In: 8th AARSE conference on earth observation for Africa's development agenda, 25-29 (October 2010, Addis Ababa, Ethiopia)
- 9 Rossi S, C J Weisstener, G Laguardia, B Kurnik, M Robustelli, S Niemeyer & N Gobron, 2008. Potential of MERIS fAPAR for drought detection. In: 2nd MERIS/(A)ATSR User Workshop, 22 - 26 September 2008, Rome, Italy, unpaginated CD-ROM, SP-666
- 10 Niemeyer S, 2008. New drought indices. Options Méditerranéennes, Series A, 80, 267-274
- 11 Horion S, H Carrão, A Singleton, P Barbosa & J Vogt, 2012. JRC experience on the development of Drought Information Systems. Europe, Africa and Latin America. EUR 25235 EN. Luxembourg (Luxembourg): Publications Office of the European Union, JRC68769 (last date accessed: 31 Jan 2013)
- 12 Smakhtin V & E L F Schipper, 2008. Droughts: The Impact of Semantics and Perceptions. Water Policy, 10: 131-143
- 13 Guswa A J, M A Celia & I Rodriguez-Iturbe, 2002. Models of soil moisture dynamics in ecohydrology: A comparative study. Water Resources. Research, 38: 1166, doi:10.1029/2001WR000826.
- 14 Clark C, 1993. How dry is a drought? Crossosoma, 19: 37-48
- 15 Ramankutty N, A T Evan, C Monfreda & J A Foley, 2008. Farming the planet: 1. Geographic distribution of global agricultural lands in the year 2000. Global Biogeochemical Cycles, 22: GB1003, doi:10.1029/2007GB002952
- 16 Bartholomé E & A S Belward, 2005. GLC2000: A new approach to global land cover mapping from Earth observation data. International Journal of Remote Sensing, 26: 1959-1977
- 17 Di Gregorio, 2005. Land Cover Classification System, Classification Concepts and User Manual. Software Version 2. FAO Environment and Natural Resources Service Series, No. 8 (last date accessed: 31 Jan 2013)
- 18 Bicheron P, M Huc, C Henry, S Bontemps & J P Lacaux, 2008. Globcover: Products Description Manual. Issue 2, Rev. 2 (last date accessed: 31 Jan 2013)
- 19 GCOS, 2007. Summary Report of the Ninth Session of the GTOS/GCOS Terrestrial Observation Panel for Climate (TOPC). WMO/TD No. 1371 (last date accessed: 31 Jan 2013)
- 20 Baret F, O Hagolle, B Geiger, P Bicheron, B Miras, M Huc, B Berthelot, F Nino, M Weiss, O Samain, J L Roujean & M Leroy, 2007. LAI, FAPAR, and FCover CYCLOPES global products derived from Vegetation. Part 1: principles of the algorithm. Remote Sensing of Environment, 110: 305-316
- 21 Sylvander S, I Albert-Grousset & P Henry, 2003. Geometrical performances of the VEGETATION products. In: IGARSS 2003, Vol. CD (Toulouse, France) IEEE
- 22 Fillol E, F Baret, M Weiss, G Dedieu, V Demarez, P Gouaux & D Ducrot, 2006. Cover fraction estimation from high resolution SPOT and medium resolution VEGETATION sensors. Validation and comparison over South-West France. In: 2nd International Colloquium on Recent Advances in Quantitative Remote Sensing, edited by J. Sobrino (Valencia, Spain: University of Valencia) 659-663 (111 MB, last date accessed: 31 Jan 2013)

- 23 Weiss M, F Baret, S Garrigues & R. Lacaze, 2007. LAI and FAPAR CYCLOPES global products derived from Vegetation. Part 2: validation and comparison with MODIS C4 products. Remote Sensing of Environment, 110: 317-331
- 24 Rudolf B, A Becker, U Schneider, A Meyer-Christoffer & M Ziese, 2010. [GPCC Status Report December 2010, Global Precipitation Climatology Centre \(GPCC\)](#) (last date accessed: 31 Jan 2013)
- 25 Phillips O L, et al., 2009. Drought Sensitivity of the Amazon Rainforest. Science, 323: 1344-1347
- 26 Maosheng Z & S W Running, 2010. Drought-induced reduction in global terrestrial net primary production from 2000 through 2009. Science, 329: 940-943
- 27 Sheffield J, K M Andreadis, E F Wood & D P Lettenmaier, 2009. Global and continental drought in the second half of the twentieth century: Severity-area-duration analysis and temporal variability of large-scale events. Journal of Climate, 22: 1962-1981
- 28 Magrin G, C Gay García, D Cruz Choque, J C Giménez, A R Moreno, G J Nagy, C Nobre & A Villamizar, 2007. [Latin America](#). Climate Change 2007: Impacts, Adaptation and Vulnerability. In: Contribution of Working Group II to the Fourth Assessment Report of the Intergovernmental Panel on Climate Change, edited by M L Parry, O F Canziani, J P Palutikof, P J van der Linden & C E Hanson (Cambridge University Press, Cambridge, UK) 581-615 (last date accessed: 31 Jan 2013)
- 29 IPCC, 2012. [Summary for Policymakers](#). In: Managing the Risks of Extreme Events and Disasters to Advance Climate Change Adaptation, edited by C B Field, V Barros, T F Stocker, D Qin, D J Dokken, K L Ebi, M D Mastrandrea, K J Mach, G-K Plattner, S K Allen, M Tignor & P M Midgley (Cambridge University Press, Cambridge, UK, and New York, NY, USA) 1-19 (last date accessed: 31 Jan 2013)
- 30 Llano M P, W Vargas & G Naumann, 2011. Climate variability in areas of the world with high production of soya beans and corn: its relationship to crop yields. Meteorological Applications, 19(4): 385-396; doi:10.1002/met.270
- 31 Wehbe M, H Eakin, R Seiler, M Vinocur, C Ávila & C Marutto, 2006. [Local perspectives on adaptation to climate change: Lessons from Mexico and Argentina](#). AIACC Working Paper No. 39, 39 pp. (last date accessed: 31 Jan 2013)
- 32 Burgan R E & R A Hartford, 1993. Monitoring vegetation greenness with satellite data. Gen. Tech. Rep. INT-297. Ogden, UT: U.S. Department of Agriculture, Forest Service, Intermountain Research Station, 13 pp.
- 33 Wilhite D & M H Glantz, 1985. Understanding the drought phenomenon: The role of definitions. Water International, 10: 111-120
- 34 Heim R R, 2002. [A review of twentieth-century drought indices used in the United States](#). Bulletin of the American Meteorological Society, 84: 1149-1165 (last date accessed: 31 Jan 2013)
- 35 Mishra A K & V P Singh, 2010. A review of drought concepts. Journal of Hydrology, 391: 202-216
- 36 McKee T B, J Nolan & J Kleist, 1993. [The relationship of drought frequency and duration to time scales](#). In: Eighth Conf. on Applied Climatology (Anaheim, CA) 179-184 (last date accessed: 31 Jan 2013)
- 37 McKee T B, J Nolan & J Kleist, 1995. [Drought monitoring with multiple time scales](#). In: Ninth Conf. on Applied Climatology (Dallas, TX, USA) 233-236 (last date accessed: 31 Jan 2013)

- 38 Wilks D S, 2005. Statistical Methods in the Atmospheric Sciences (International Geophysics, 2nd edition, Academic Press) 648 pp.
- 39 Hayes M J, D A Wilhite, M Svoboda & O Vanyarkho, 1999. [Monitoring the 1996 drought using the Standardized Precipitation Index](#). Bulletin of the American Meteorological Society, 80: 429-438 (last date accessed: 31 Jan 2013)
- 40 Minetti J, W Vargas, G Casagrande, G Vergara & L Acuña, 2004. [La Sequía 2003-2004 en Argentina](#). In: X Reunión Argentina y IV Latinoamericana de Agrometeorología Agrometeorología y seguridad alimentaria en América Latina (AADA, Mar del Plata, Argentina, 13 al 15 de Octubre de 2004) (last date accessed: 31 Jan 2013)
- 41 Alessandro A P, 2008. [Anomalies of the atmospheric circulation at 500 and 1000 hpa associated with the dry period in Argentina from January 2003 to March 2004](#). Revista Brasileira de Meteorologia, 23: 12-29 (last date accessed: 31 Jan 2013)